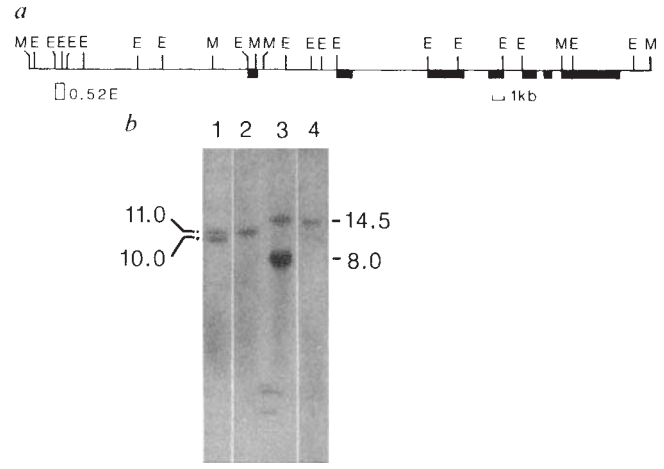

Fig. 3 DNA analysis to detect *abl* rearrangements. *a*, Restriction map for the 5′ region of c-*abl* located on chromosome 9 band q34. Closed boxes, regions homologous to v-*abl*; open box, the probe 0.52E. Abbreviations for enzyme sites are as in Fig. 1*a*. Scale bar, 1 kb. *b*, DNA from F.Y. (lane 1 and 3) or Bri-7 (lanes 2 and 4) was digested with Bg1II (lanes 1 and 2) or *Bam*HI (lanes 3 and 4) and treated as in Fig. 1*b*. The blot was hybridized to the upstream *abl* probe labelled by the random primer method[19]. Sizes of fragments hybridizing in kb.

originally in Ph$^+$ CML while the other appears to involve sequences outside the designated 5.8-kb *bcr*. Because the latter mechanism has not been detected in a large series of chronic phase Ph$^+$ leukaemia (CML) cases, there appears to be some association between these two mechanisms and disease status. Note that we have not determined whether another region of the *bcr* (or *phl*) gene on chromosome 22, might be involved in this translocation. Interestingly, we have recently screened 13 cases of ALL without the Ph chromosome and identified one which appears to express a normal (p145) sized *abl* related protein with enhanced PTK activity or elevated level of the protein (C. Girdham and K.K.K., data not shown). This may represent a third mechanism for the activation of the c-*abl* proto-oncogene.

It has been suggested that Ph$^+$, bcr$^+$ ALL, which produces an 8.7-kb aberrant *bcr-abl* transcript can be considered to be Ph$^+$ CML in which lymphoid blast crisis has occurred after an undetected chronic phase arising in multipotential progenitor cells[6] (see also refs 4, 5). Our DNA data on patient F.B. which shows rearrangement in the *bcr* and the cellular expression of p210 is consistent with this hypothesis. Ph$^+$, bcr$^-$ ALL might then represent *de novo* B lymphocyte precursor ALL. It is uncertain at present, owing to the small number of cases in our study, whether Ph$^+$, bcr$^-$ ALLs which produce the novel c-*abl* p190 protein are indeed clinically distinct from Ph$^+$, bcr$^+$ ALL. This can perhaps be assessed by testing for c-*abl* p190 PTK in remission and by clinical follow up of remission duration and disease evolution of relapse in a larger series of patients. What is clear is that this group includes adults as well as children, in contrast to previous studies which suggested that Ph$^+$, bcr$^-$ ALL is primarily a childhood disorder[7,15]. A summary of the Ph$^+$ ALL cases in our study is shown in Table 1.

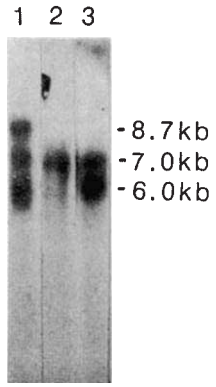

Fig. 4 RNA analysis for altered *abl* mRNA sequences. Poly(A)$^+$ RNAs (6–10 μg) were analysed by electrophoresis, blotting and hybridized to a v-*abl* kinase domain probe. RNAs were purified from K562, a bcr$^+$ cell line derived from a patient with CML in blast crisis (lane 1); cells from patient A.E. (lane 2); and KGl, a myeloid cell line with no Ph involvement (lane 3). RNA sizes in kb as determined from size markers.
Methods. RNA was isolated from cells using the guanidinium thiocyanate method followed by centrifugation through CsCl[20] and enriched for poly(A)$^+$ RNA by oligo-dT chromatography[21]. The RNA was denatured, electrophoresed through a 6% formaldehyde, 0.8% agarose gel[22], transferred to Genescreen Plus (NEN) and immobilized by exposure to a UV light source for 5 min followed by baking for 2 h at 80 °C. The blot was then hybridized to a nick-translated v-*abl* probe[14] and autoradiographed.

We thank U. Glass, B. R. Reeves, S. Feary, H. Davies and D. Sheer for help with cytogenetic information; S. M. Pegram, J. E. Gillies and M. K. K. Shivji for technical assistance; Dr J. Goldman for helpful discussion, and Miss G. Parkins and Mrs J. Needham for help in preparation of the manuscript. This work was supported by the Leukaemia Research Fund of Great Britain and the MRC.

Received 9 October; accepted 16 December 1986.

1. Groffen, J. *et al. Cell* **36**, 93-99 (1984).
2. Konopka, J. B. & Witte, O. N. *Molec. cell. Biol.* **5**, 3116-3123 (1985).
3. Ben-Neriah, Y., Daley, G. Q., Mes-Masson, A-M., Witte, O. N. & Baltimore, D. *Science* **233**, 212-214 (1986).
4. Greaves, M. F. *Chronic Granulocytic Leukaemia* (ed. Shaw, M. T.) 15-47 (Praeger, New York, 1982).
5. Catovsky, D. *Br. J. Haemat.* **42**, 493-498 (1979).
6. De Klein, A. *et al. Blood* **6**, 1369-1375 (1986).
7. Erikson, J. *et al. Proc. natn. Acad. Sci. U.S.A.* **83**, 1807-1811 (1986).
8. Greaves, M. F., Janossy, G., Peto, J. & Kay, H. *Br. J. Haemat.* **48**, 179-197 (1981).
9. Minowada, J., Koshiba, H., Janossy, G., Greaves, M. F. & Bollum, F. J. *Leuk. Res.* **3**, 261-266 (1979).
10. Konopka, J. B., Watanabe, S. M. & Witte, O. N. *Cell* **37**, 1035-1042 (1984).
11. Heath, J. K., Mahadevan, L. & Foulkes, J. G. *EMBO J.* **5**, 1809-1814 (1986).
12. Heisterkamp, N. *et al. Nature* **306**, 239-242 (1983).
13. Grosveld, G. *et al. Molec. cell. Biol.* **6**, 607-616 (1986).
14. Shtivelman, E., Lifshitz, B., Gale, R. P. & Canaani, E. *Nature* **315**, 550-554 (1985).
15. Rodenhuis, S., Smets, L. A., Slater, R. M., Behrendt, H. & Veerman, A. *New Engl. J. Med.* **313**, 51 (1985).
16. Southern, E. M. *J. molec. Biol.* **98**, 503-517 (1975).
17. Konopka, J. B. *et al. J. Virol.* **51**, 223-232 (1984).
18. Laemmli, U.K. *Nature* **227**, 680-685 (1970).
19. Feinberg, A. P. & Vogelstein, B. *Analyt. Biochem.* **137**, 266-267 (1984).
20. Wiedemann, L. M., Burns, J. H. & Birnie, G. D. *EMBO J.* **2**, 9-13 (1983).
21. Aviv, H. & Leder, P. *Proc. natn. Acad. Sci. U.S.A.* **69**, 1408-1412 (1972).
22. Lehrach, H., Diamond, D., Wozney, J. M. & Boedtker, T. *Biochemistry* **16**, 4743-4751 (1977).

Rapid rotation of flagellar bundles in swimming bacteria

Graeme Lowe, Markus Meister & Howard C. Berg*

Division of Biology 216-76, California Institute of Technology, Pasadena, California 91125, USA

A bacterial flagellum is driven by a reversible rotary motor[1–3]. The power input is determined by protonmotive force and proton flux, the power output by torque and speed: interrelationships between these parameters provide important clues to motor mechanisms. Here we describe the relationship between torque and speed at constant protonmotive force. The measurements are analogous to those that could be made by plugging an electric motor into a constant-voltage outlet, varying the external load, and determining the torque delivered at different speeds. We used suspensions of metabolizing cells of a motile *Streptococcus*, varied the external load by changing the viscosity of the medium, determined motor speed from the frequency of vibration of the cell body, and inferred motor torque from the rate of body rotation. The flagellar bundles rotate more rapidly than formerly supposed, at rates that increase linearly with temperature. The torque delivered by the flagellar motor drops linearly with speed. At high speed, the torque-generating cycle associated with the transfer of one proton appears to dissipate free energy in a series of small steps.

The helical bundle of a swimming bacterium generates thrust, and the cell translates at a velocity at which this force is balanced

* Present address: Department of Cellular and Developmental Biology, Harvard University, Cambridge, Massachusetts 02138, USA.

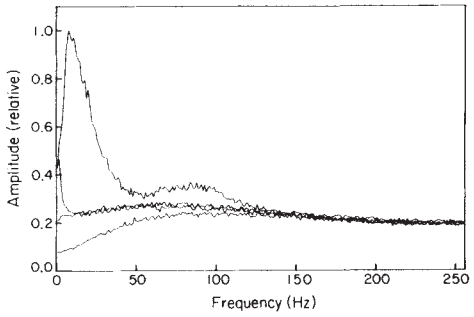

Fig. 1 Amplitude spectra of swimming cells of *Streptococcus* (top curve), of de-energized cells moving at the speed of the swimming cells (second curve), of de-energized cells undergoing Brownian movement (third curve), and of the background illumination at the same total light intensity (bottom curve).

Methods. Cells of a smooth-swimming mutant, SM197, were grown at 35 °C in KTY medium[2], collected at late exponential phase, washed twice by centrifugation (480*g*, 6 min) in an equal volume of 0.1 M sodium phosphate (*p*H 7.5), 0.2 M KCl, 0.1 mM EDTA, 0.01 M D-glucose, and then resuspended in this medium at a density of $\sim 4 \times 10^8$ cells ml^{-1}. An aliquot of this suspension was drawn into a flow chamber[22] (0.4 mm deep) and examined at 22 °C under an inverse phase contrast microscope (see below), yielding the spectrum shown in the top curve (mean swimming speed ± s.e.m., 15.7 ± 1.1 μm s^{-1} for 17 cells, as judged from slow-speed playback of a video recording[23]). Another aliquot was de-energized by the addition of the uncoupler FCCP (trifluoromethoxycarbonylcyanide phenylhydrazone, 10 μg ml^{-1}) and either drawn through the chamber at a speed of 14.4 μm s^{-1} (measured at the middle of the chamber), yielding the spectrum shown in the second curve, or examined when stationary, yielding the spectrum shown in the third curve. The microscope (Nikon S-Ke) was equipped with a 100 W tungsten-halogen lamp (type FCR, driven by a constant-voltage d.c. power supply), a heat-transmitting mirror (Optical Industries 03MCS007), a CF BM ×40 objective, a ×20 eyepiece, a $\frac{1}{2}\times$ PFM photomicrographic attachment, and a photomultiplier tube (RCA 4886, run at 300 V). The focal plane was located midway between the top and bottom windows of the flow chamber to minimize wall effects. The diameter of the photocathode (1.8 cm), referred to the focal plane, was ~39 μm. The output of the photomultiplier was passed through a current-to-voltage converter (10^7 Ω feedback), a difference amplifier (to remove the d.c. offset and amplify the a.c. signal), a double-pole low-pass filter, and a single-pole high-pass filter. The 3 dB cutoff points of these filters were set at 200 and 72 Hz, respectively. A 12-bit analogue-to-digital converter sampled data at 512 points s^{-1} for one-second intervals and a PDP-11/34 computer computed and averaged the corresponding power spectra (400 times for the data shown). The signals arose from lateral motion of images on the photocathode, which was exposed to light from only a small region of the flow chamber, and which when scanned with the image of a cell that was stuck to glass, was found to have an output (signal less background) that rose and fell 3 or 4 times across a diameter, varying in amplitude by as much as 50%. Contributions from out-of-focus components of the images were significant, as useful spectra could be obtained on moving the plane of focus beyond the limits of the flow chamber. The basic features of the spectra, including sidebands due to non-linearities encountered with larger displacements (see text), could be reproduced by mounting the detector on the tracking microscope[24], suspending de-energized cells in the tracking chamber, and moving it sinusoidally with the tracker drive. Much larger signals were obtained on moving the tracking chamber sideways than up and down. De-energized cells and monodisperse polystyrene latex spheres (1.3 μm diameter) gave identical spectra.

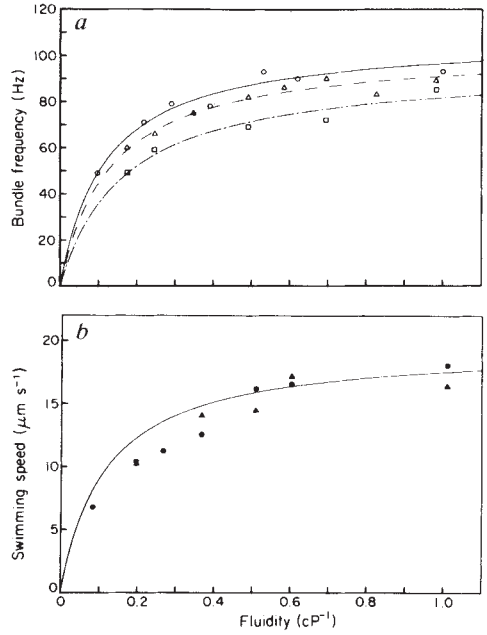

Fig. 2 Bundle frequencies (*a*) and swimming speeds (*b*) of *Streptococcus* as a function of the fluidity of the medium. The different symbols refer to cells from different cultures. The values shown at each point are means for the cell population determined from the power spectrum or the tracking data, respectively. In either case, the spread (s.d. divided by the mean) was about 25%. The fits to the data in *a* are shown in Fig. 3. The solid curve in *b* is the solid curve in *a*, redrawn and scaled to match approximately the swimming speeds at high fluidity.

Methods. To measure bundle frequencies, cells of strain SM197 were grown, collected, washed as described in Fig. 1. Then (open circles) cells were resuspended at 80 times the density at collection. An aliquot was mixed with 9 vols of Ficoll 400 solution of known concentration. Alternatively (open triangles and open squares), cells were pelleted once, as before, and resuspended in a solution of Ficoll in KTY medium. All spectra were taken as described in Fig. 1, except in a shallower chamber (0.15 mm deep)[23]. Ficoll standards were prepared by serial dilution of a 20% w/v stock prepared in the medium in which the cells were suspended. The viscosities of these solutions were measured at 22 °C in a Cannon-Ubbelohde viscometer (viscometer constant 8.13×10^5 cm^2 s^{-2}). The same stock was used to prepare all the Ficoll solutions. The position of the centre of the high-frequency peak was found as follows. The power spectrum for non-motile cells was smoothed with a cubic spline procedure[25] and subtracted from the power spectrum for the swimming cells. The difference spectrum was smoothed in the same way, and its low-frequency peak was fitted by a curve generated by computer simulation (see text). This curve was subtracted out, and the centre of the remaining (high-frequency) peak was found by eye. To measure swimming speeds, cells of the wild-type strain V4051 (ref. 26) were grown, collected and washed as described in Fig. 1, and then resuspended at 2.5 times the density at collection. An aliquot was mixed with 50 volumes of a solution of Ficoll of known concentration, and the swimming speeds of 20–30 cells were found by tracking[24]. The following data (mean ±s.d., unless otherwise noted) were obtained for a population of 60 bacteria in the absence of Ficoll (compare ref. 27, Table 1): speed 16.8 ± 3.7 μm s^{-1} (mean ±s.e.m.), tumble length 0.18 ± 0.07 s, run length 1.71 ± 0.90 s, change in direction from run to run $63 \pm 14°$, and change in direction during runs $26 \pm 8°$. The run-tumble statistics also were Poisson.

by viscous drag on the body; the bundle also generates torque, and the body counter-rotates (or rolls). If the longitudinal axes of the bundle and the cell body are not collinear, then the image of the body wobbles from side to side. If there is a net imbalance in the forces perpendicular to the axis of the helix, for example, if the bundle does not contain an integral number of wavelengths[4], then the cell body also vibrates (or gyrates) at the rotation frequency of the bundle. The presence of such motion was postulated long ago by Reichert[5], who referred to it as *die Trichterbewegung*, or funnel movement[6].

We measured these frequencies by projecting the images of swimming cells onto the photocathode of a photomultiplier tube whose sensitivity is spatially inhomogenous. The output was passed through a bandpass filter and the power spectral density was computed with the fast Fourier transform. The spectra of many successive one-second data blocks were averaged. The

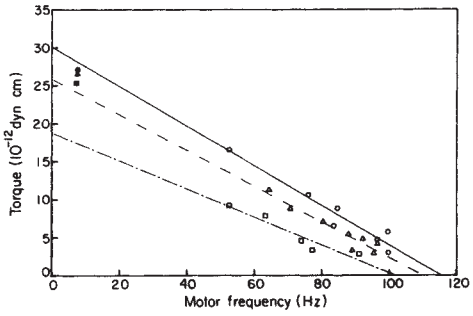

Fig. 3 Torque of the flagellar motor of *Streptococcus* as a function of speed. The open symbols are values derived from the data of Fig. 2*a*. The lines are least-squares fits to these data. The closed symbols are values derived from experiments on cells tethered by a flagellar filament[11].

Methods. For swimming cells, the torque exerted by the bundle on the cell body is given by the product of the body-roll frequency, the viscosity of the medium, and a geometrical factor that depends on the shape of the cell and its axis of rotation. We approximated the cell body as a cylinder of length 3.27 μm and width 1.27 μm rolling about an axis that intersects the cylinder axis 1.09 μm from one end of the cell at an angle of 22°. Cell sizes were determined from photomicrographs of cells that had settled on a glass surface, whereas other parameters related to the geometry were estimated by inspecting the trajectory of several cells on the video record. The corresponding drag coefficient was computed from published formulae[28,29]. No correction was made for the additional viscous drag on the body due to the counter-rotation of the flagellar bundle or for loss of torque due to interactions of flagella within the bundle; the latter assumption is justified by the observation that free hooks[2] or flagellar stubs[7] spin at rates comparable to those of flagellar bundles. We visualized the flagellar filaments with a modified Ryu stain[30] and found an average of 3.5 ± 0.2 flagella per cell, all of which were assumed to join in a single bundle. For tethered cells, cells from three cultures were prepared as described in Fig. 1 and tethered to a silanized cover slip[11]. We approximated the cell body as a cylinder of length 3.04 μm and width 1.36 μm spinning about an axis perpendicular to the cylinder axis 0.32 μm away from the centre of the cell. No correction was made for the additional viscous drag due to the proximity of the cover slip[31].

top curve of Fig. 1 shows the amplitude of this spectrum (the square-root of the power spectrum) obtained from a field of smooth-swimming cells of *Streptococcus*; the low-frequency peak is due to the roll of the cell body and the high-frequency peak to its funnel movement. The other spectra in Fig. 1 characterize noise arising from changes in the number of cells imaged on the detector, Brownian movement and photoelectron statistics.

To interpret these spectra better, we simulated the measurements by computer, moving a vibrating spot across a detector with a radial gaussian sensitivity and filtering the output. We concluded from this analysis that the low-frequency peak (Fig. 1) is skewed toward high frequencies because of harmonics of the body-roll frequency that arise from the nonlinear relation between displacement and detector output at large wobble amplitudes. The high-frequency peak, on the other hand, although broadened somewhat by sidebands generated by mixing with the low-frequency signal, remains centred at the mean bundle frequency, provided (as in Fig. 1) that the two peaks do not considerably overlap. Both peaks are broadened and smoothed by variations over the cell population[7].

The correct body-roll frequency corresponding to each amplitude spectrum was determined by examining video recordings made of the same cell suspensions. An average was computed from the wobble frequencies of all the cells in a video field, as measured by eye and stopwatch during slow-speed playback. For the culture used in the experiments of Fig. 1, the body-roll frequency was 6.7 ± 2.4 Hz (mean ±s.d. for 20 cells). Given a bundle frequency of about 95 Hz (Fig. 1), this yields a value for

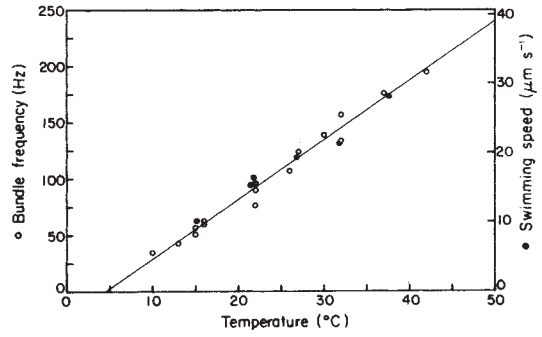

Fig. 4 Bundle frequencies (○) and swimming speeds (●) of *Streptococcus* as a function of temperature. The values shown are the means for the cell population, determined at each point from the power spectrum or the tracking data, respectively. In either case, the spread was about 25%. The temperature was controlled as described previously[10]. Other conditions were as in Fig. 2 (with cells prepared in phosphate buffer). The line is a least-squares fit to the bundle-frequency data. The swimming-speed scale was adjusted so that the swimming-speed data fell along the same line.

the speed of the flagellar motor relative to the cell body of about 100 Hz.

Figure 2 shows the dependence of bundle frequency and swimming speed on the fluidity of the medium, adjusted by addition of Ficoll, a highly branched viscous agent whose solutions show newtonian properties[8]. A tenfold increase in viscosity was required to halve the bundle frequency. Swimming speeds were closely correlated with bundle frequencies, but they were slightly lower at higher viscosities: the ratio of swimming speed to bundle frequency decreased from 0.18 ± 0.01 μm to 0.15 ± 0.01 μm for the data shown. A possible explanation for this trend is that the bundle winds up slightly as the torque increases, decreasing its propulsive efficiency. We also measured bundle frequencies of *Streptococcus* as a function of fluidity using methylcellulose and found that the frequencies decreased monotonically with increasing viscosity (data not shown). Thus, increases in swimming speed observed on the addition of small amounts of this agent[9] must arise from enhancement of the efficiency of flagellar propulsion, as argued previously[8], not from changes in the speed of the flagellar motors.

Figure 3 shows the torque generated by the flagellar motor as a function of its rotation rate. The open symbols are a different representation of the data of Fig. 2*a*: their position on the abscissa is the sum of the body-roll and bundle frequencies, equal to the motor rotation frequency, whereas their position on the ordinate is proportional to the product of the body-roll frequency and the viscosity of the medium. The proportionality constant is determined by a geometrical drag factor and the number of filaments per bundle. The same constant was assumed for all the experiments on swimming cells. For the three cultures, the torque appears to drop linearly with increasing speed, although the relationship varies somewhat from culture to culture. The closed symbols represent the torque for tethered cells, calculated in the same fashion, but with a different geometrical drag factor. These torques correspond well to the linear extrapolation of the data for swimming cells. Note that the ratio of the two drag factors, and thus the position on the ordinate of the closed symbols relative to the open symbols, is subject to considerable uncertainty, probably up to 40%. The implications of Fig. 3 for the mechanism of torque generation are discussed below.

Figure 4 shows the dependence of bundle frequency (open symbols) and swimming speed (closed symbols) of *Streptococcus* on temperature. Both increase linearly over the range 10 to 40 °C. To check for a possible temperature dependence of the protonmotive force, we tethered cells from the culture used for

the bundle-frequency measurements. Their torques were compared at 9.3, 16.0, 22.0, 27.8 and 31.6 °C and found to fall in the ratios 0.7, 0.95, 1.00, 1.02 and 1.04, respectively (torques for each of 14 cells were scaled to the torque at 22 °C and then averaged; the standard deviation for the population was ~0.05; the mean speed at 22 °C was 6.3 Hz). Artificially energized cells generate a torque that is essentially independent of temperature over the range 4–38 °C[10]. Assuming a linear dependence of torque on protonmotive force[10,11], we conclude that the protonmotive force of metabolizing cells increases by at most 10% over the temperature range 16–32 °C. Over this range, the bundle frequencies of the swimming cells increased by a factor of 2.4 (Fig. 4). A linear dependence of swimming speed on temperature has been observed for *Escherichia coli* using number-fluctuation spectroscopy[12] and cinematography[13]. Similar results were obtained for *Salmonella typhimurium* by recording motility tracks[14].

We also measured the bundle frequencies and swimming speeds of *E. coli*. The mean bundle frequency of a smooth-swimming strain (HCB437) grown at 35 °C on glycerol in a minimal salts medium, collected at mid-exponential phase, and then studied in motility medium[15] at 22 °C—these were the conditions used for the measurements of rotational frequencies of hooks described earlier (mean ± s.d. for 20 cells 104 ± 29 Hz)[2]—gave a result in the same range, 113 Hz. The mean bundle frequency for these cells was higher at 32 °C, 156 Hz. We also determined mean bundle frequencies for cells grown at 35 °C in tryptone broth and collected at mid-exponential phase. These frequencies were higher still, 191 Hz at 22 °C, and 268 Hz at 32 °C. All these measurements were made near the open edge of the chamber[8] to ensure that the cells were well oxygenated. Cells of wild-type strain AW405 (ref. 16) were grown on tryptone broth and tracked at 32 °C in motility medium containing varying amounts of Ficoll. The dependence of swimming speed on fluidity was essentially identical to that observed for *Streptococcus* (Fig. 2*b*), except that the swimming speeds were higher (mean ±s.e.m. for 79 cells at fluidity 1.25 cP^{-1}, 36.4 ± 1.0 $\mu m\ s^{-1}$).

What can these measurements tell us about the physics of flagellar propulsion? The torque of the motor drops monotonically with increasing speed, and the relationship appears to be approximately linear over a wide range (Fig. 3). These results do not favour a mechanism by which the motor runs at constant power: in that case the torque would be inversely proportional to speed, and the fits would be hyperbolic. This conclusion is reinforced by two additional observations, namely, that the torque generated by a tethered cell is approximately constant for speeds from ~10 Hz to stall (ref. 11 and M.M., H.C.B., in preparation), and that the speed observed with hooks approximates the speed observed with flagellar bundles. The frictional drag coefficient of a hook is very much smaller than that of a filament in a bundle. Therefore, the intercepts of the linear fits with the axes of Fig. 3 are confirmed experimentally.

In the framework of thermodynamics, one can treat the flagellar motor as a system coupling two flows: the flux of protons and the rotation of the rotor. If the system operates close to thermodynamic equilibrium, then the flows are linear functions of the pair of conjugate driving forces, namely, the protonmotive force and the torque acting on the rotor[17]. When the protonmotive force is held constant, as it was in the measurements of Fig. 3, torque should decrease linearly with speed. Chemical processes occur close to equilibrium when the difference in the free energies of reactants and products (dissipated as heat) is small compared to kT, where k is the Boltzmann constant and T is the absolute temperature. The observed linear relationship between torque and speed appears to extend to the point where the motor generates essentially no torque and, thus, performs no mechanical work. At this speed, all the free energy available per proton (~8 kT) is dissipated by processes internal to the motor. The motor could still operate in the linear regime if the torque-generating cycle associated with the transfer of one proton involved a series of many reactions, each of which entailed only a small free energy loss.

A mechanism that has this feature has been proposed by Läuger[18], where protons are translocated from the external medium into the cytoplasm along binding sites at the intersections between rows of ligands on the faces of the M and S rings. The two sets of rows are tilted with respect to each other, so proton movement is coupled to motor rotation. Läuger discussed the operation of this device at low speeds and suggested that the torque should be independent of speed below 10 Hz. At the much higher speeds observed in swimming cells, finite proton transfer rates might lead to considerable dissipation of free energy conduction along the ligand chain and thus limit the torque. If each row contains 10 or more sites, the torque might still vary linearly with speed.

In a model proposed by Berg and Khan[19], a single torque-generating step uses all the electrochemical energy of a proton and stores it as elastic energy in a spring. This process becomes rate-limiting at high speeds and accounts for all the internal dissipation. A preliminary analysis of this mechanism at steady state predicts a nonlinear dependence of torque on speed that is inconsistent with the data of Fig. 3. However, the model can be altered successfully by assuming that protons reach the rotor by stepping along a series of sites in a membrane channel, provided that the latter process is rate-limiting at high speeds.

An approximately linear torque-speed relationship can be obtained from mechanisms that work far from thermodynamic equilibrium, but only explicit construction. An example is the model proposed by Oosawa and Hayashi[20], in which proton transfer and rotation are loosely coupled. Measurements of torque at high speed place strict requirements on all models for the bacterial motor and deserve more attention.

We thank R. D. Smyth for help with the tracking experiments, D. F. Blair for discussions, and E. M. Purcell for comments on the manuscript. Development of the technology was inspired by the light-scattering experiments of C. Ascoli and C. Frediani and their colleagues[21]. This work was supported by grants from the US NSF (DMB8518257) and the Gustavus and Louise Pfeiffer Foundation. G.L. and M.M. were recipients of Earle C. Anthony Fellowships.

Received 14 October; accepted 11 December 1986.

1. Berg, H. C. & Anderson, R. A. *Nature* **245**, 380–382 (1973).
2. Berg, H. C., Manson, M. D. & Conley, M. P. *Symp. Soc. exp. Biol.* **35**, 1–31 (1982).
3. Macnab, R. M. & Aizawa, S.-I. *A. Rev. Biophys. Bioeng.* **13**, 51–83 (1984).
4. Berg, H. C. *Random Walks in Biology*, 78–79 (Princeton University Press, New Jersey, 1983).
5. Reichert, K. *Zentr. Bakt. Parasitenkde Ab. 1 Orig.* **51**, 14–94 (1909).
6. Berg, H. C. *A. Rev. Biophys. Bioeng.* **4**, 119–136 (1975).
7. Lowe, G. thesis Calif. Inst. Technol. (1987).
8. Berg, H. C. & Turner, L. *Nature* **278**, 349–351 (1979).
9. Schneider, W. R. & Doetsch, R. N. *J. Bact.* **117**, 696–701 (1974).
10. Khan, S. & Berg, H. C. *Cell* **32**, 913–919 (1983).
11. Manson, M. D., Tedesco, P. M. & Berg, H. C. *J. molec. Biol.* **138**, 541–561 (1980).
12. Banks, G., Schaefer, D. W. & Alpert, S. S. *Biophys. J.* **15**, 253–261 (1975).
13. Maeda, K., Imae, Y., Shioi, J.-I. & Oosawa, F. *J. Bact.* **127**, 1039–1046 (1976).
14. Miller, J. B. & Koshland, D. E., Jr *J. molec. Biol.* **111**, 183–201 (1977).
15. Ishihara, A., Segall, J. E., Block, S. M. & Berg, H. C. *J. Bact.* **155**, 228–237 (1983).
16. Armstrong, J. B., Adler, J. & Dahl, M. M. *J. Bact.* **93**, 390–398 (1967).
17. Prigogine, I. *Introduction to Thermodynamics of Irreversible Processes* 2nd edn (Interscience, New York, 1961).
18. Läuger, P. *Nature* **268**, 360–362 (1977).
19. Berg, H. C. & Khan, S. in *Motility and Recognition in Cell Biology* (eds Sund, H. & Veeger, C.) 486–497 (de Gruyer, Berlin, 1983).
20. Oosawa, F. & Hayashi, S. *J. Phys. Soc. Japan* **52**, 4019–4028 (1983).
21. Angelini, F., Ascoli, C., Frediani, C. & Petracchi, D. *Biophys. J.* **50**, 929–936 (1986).
22. Berg, H. C. & Block, S. M. *J. gen. Microbiol.* **130**, 2915–2920 (1984).
23. Segall, J. E., Ishihara, A. & Berg, H. C. *J. Bact.* **161**, 51–65 (1985).
24. Berg, H. C. *Adv. opt. Elect. Micros.* **7**, 1–15 (1978).
25. Reinsch, C. H. *Numer. Math.* **10**, 177–183 (1967).
26. Van der Drift, C., Duiverman, J., Bexkens, H. & Krijnen, A. *J. Bact.* **124**, 1142–1147 (1975).
27. Berg, H. C. & Brown, D. A. *Nature* **239**, 500–504 (1972).
28. Tirado, M. M. & de la Torre, J. G. *J. chem. Phys.* **71**, 2581–2587 (1979).
29. Tirado, M. M. & de la Torre, J. G. *J. chem. Phys.* **73**, 1986–1993 (1980).
30. Heimbrook, M. E., Wang, W. L. L. & Campbell, G. *Abstracts of the Annual Meeting of the American Society for Microbiology, 1986*, 240 (American Society for Microbiology, Washington DC, 1986).
31. Berg, H. C. in *Cell Motility* Vol. 3C (eds Goldman, R., Pollard, T. & Rosenbaum, J.) 47–56 (Cold Spring Harbor Laboratory, New York, 1976).